Human Molecular Genetics, 2001, Vol. 10, No. 21 **2341–2351**

Oligomerization of polyalanine expanded PABPN1 facilitates nuclear protein aggregation that is associated with cell death

Xueping Fan, Patrick Dion, Janet Laganiere, Bernard Brais[1] and Guy A. Rouleau*

Center for Research in Neuroscience, McGill University, and the McGill University Health Center, 1650 Cedar Avenue, Montreal, Quebec H3G 1A4, Canada and [1]Centre de recherche du CHUM, Hôpital Notre-Dame, Université de Montréal, 1560 Sherbrooke East, Montreal, Quebec H2L 4M1, Canada

Received May 14, 2001; Revised and Accepted June 27, 2001

Oculopharyngeal muscular dystrophy (OPMD) is an adult-onset disorder characterized by progressive eyelid drooping, swallowing difficulties and proximal limb weakness. The autosomal dominant form of this disease is caused by short expansions of a $(GCG)_6$ repeat to $(GCG)_{8–13}$ in the PABPN1 gene, which results in the expansion of a polyalanine stretch from 10 to 12–17 alanines in the N-terminus of the protein. Mutated PABPN1 (mPABPN1) is able to induce nuclear protein aggregation and form filamentous nuclear inclusions, which are the pathological hallmarks of OPMD. PABPN1, when bound to poly(A) RNA, forms both linear filaments and discrete-sized, compact oligomeric particles *in vitro*. In the absence of poly(A) RNA, PABPN1 can form oligomers. Here we report that: (i) oligomerization of PABPN1 is mediated by two potential oligomerization domains (ODs); (ii) inactivating oligomerization of mPABPN1 by deletions of 6–8 amino acids in either of the ODs prevents nuclear protein aggregation; (iii) expression of mPABPN1 in COS-7 cells is associated with cell death; and (iv) preventing nuclear protein aggregation by inactivating oligomerization of mPABPN1 significantly reduces cell death. These findings suggest that oligomerization of PABPN1 plays a crucial role in the formation of OPMD nuclear protein aggregation, while the expanded polyalanine stretch is necessary but not sufficient to induce OPMD protein aggregation, and that the nuclear protein aggregation might be toxic and cause cell death. These observations also imply that inactivation of oligomerization of mPABPN1 might be a useful therapeutic strategy for OPMD.

INTRODUCTION

Autosomal dominant oculopharyngeal muscular dystrophy (OPMD) is an adult-onset disease that presents in the fifth or sixth decade. The disease is characterized by progressive eyelid drooping (ptosis), swallowing difficulties (dysphagia) and proximal limb weakness (1). OPMD has a worldwide distribution (2–6), but is particularly frequent in the French-Canadian population (1). Pathological studies showed the presence of unique intranuclear filamentous inclusions in skeletal muscle fibers of OPMD patients (7,8). Under the electron microscope, the OPMD intranuclear inclusions are seen as tubular filaments with an outer diameter of 8.5 nm, an inner diameter of 3 nm and a length of <0.25 μm (7,8).

The OPMD locus was mapped by linkage analysis to chromosome 14q11.1 (9–11) and the gene was identified as PABPN1, which encodes for the poly(A) binding protein, nuclear 1 (PABPN1, PABP2, PAB II) (12). Dominant OPMD is caused by the expansion of a short GCG trinucleotide repeat in the PABPN1 gene. The normal PABPN1 gene has a $(GCG)_6$ trinucleotide repeat coding for a polyalanine stretch at its 5′ end while in OPMD patients this $(GCG)_6$ repeat is expanded to $(GCG)_{8–13}$. Due to the presence of GCA GCA GCA GCG coding sequence adjacent to the $(GCG)_6$ repeat, the wild-type PABPN1 has a 10-alanine stretch in its N-terminus, while the mutant proteins have 12–17 alanines.

In addition to OPMD, at least five other diseases are associated with alanine stretch expansions in the disease gene products. Synpolydactily (SPD) is caused by an alanine stretch expansion from 15 to 22–25 in the HOXD13 (13), while cleidocranial dysplasia (CCD) is associated with an expansion from 17 to 27 alanines in CBFA1 protein (14). The alanine stretch lengthening from 15 to 25 in ZIC2 protein results in holoprosencephaly (HPE) (15), whereas, the ones expanded from 15 to 22–33 in HOXA13 protein and from 14 to 24 in FOXL2 protein cause hand-foot-genital syndrome (HFGS) (16) and type II blepharophimosis/ptosis/epicanthus (type II BPES) (17), respectively. Among these alanine-expanded proteins, mutated PABPN1 (mPABPN1) is the only one that is reported to induce the formation of intranuclear inclusions. OPMD intranuclear inclusions are similar to those found in a number of inherited neurodegenerative diseases caused by mutated proteins with an expanded polyglutamine (polyQ) stretch encoded by a CAG repeat. The mutant form of each protein typically bears a polyQ tract greater than 40 residues,

*To whom correspondence should be addressed at: Room L7-224, Montreal General Hospital, 1650 Cedar Avenue, Montreal, Quebec H3G 1A4, Canada. Tel: +1 514 934 8094; Fax: +1 514 934 8265; Email: mi32@musica.mcgill.ca

whereas the wild-type protein may contain approximately 20 glutamines (18). This group of disorders includes Huntington's disease (HD) (19), spinobulbar muscular atrophy (SBMA) (20), dentatorubral pallidoluysian atrophy (DRPLA) (21,22) and the spinocerebellar ataxia (SCA) types 1, 2, 3, 6 and 7 (23–29). In most of these diseases, the mutant protein accumulates as inclusions in the nucleus of a neuronal cell population specific to each disease. The neurons containing these aggregates eventually undergo cell death, with a corresponding decrease in the brain mass in the affected individual (18).

PABPN1 has 306 amino acids, and comprises an alanine stretch and a proline-rich region (PRR) in the N-terminus, a putative ribonucleoprotein (RNP)-type RNA binding domain in the central region and an arginine-rich C-terminus. PABPN1 is an abundant nuclear protein that binds with high affinity to the poly(A) tail of mRNA, and is involved in mRNA polyadenylation (30), a two-step reaction whereby endonucleolytic cleavage of the nascent mRNA transcript is followed by the addition of approximately 250 adenylate residues to the upstream cleavage product (reviewed in 31–33). Poly(A) tail synthesis is catalyzed by poly(A) polymerase through interaction with CPSF, the cleavage and polyadenylation specificity factor. However, this process is slow and inefficient, and the length of poly(A) tail is poorly controlled. Adding PABPN1 to this reaction will stimulate processive poly(A) addition and control the size of the tail to be ~250 nucleotides in length (30,34,35).

The PABPN1 RNA binding domain mediates its specific binding to the poly(A) tail of mRNA (36). Poly(A)-bound PABPN1 forms both linear filaments and discrete-sized, compact oligomeric particles *in vitro* (37). Titration and gel retardation assays indicated that 12 adenylate residues are required for high affinity RNA binding, and the packing density on the poly(A) tail is approximately 15 adenylate residues per PABPN1 molecule (36). However, PABPN1 tends to form oligomers even in the absence of mRNA (38).

PABPN1 has been identified as a component of the filamentous inclusions present in the nuclei of OPMD muscle fibers (39–41). Expression of mPABPN1 in COS-7 cells induces the formation of intranuclear protein aggregation (42). The alanine stretches in the wild-type transcription factors HOXD13, CBFA1, ZIC2, HOXA13 and FOXL2 range from 14 to 17 alanines, and the diseases caused by polyalanine expansions in these genes require 22 or more alanines. However, the 12-alanine stretch in PABPN1 induces protein aggregation and causes dominant OPMD symptoms (12). These differences suggest that there must be other characteristics of PABPN1 that promote or facilitate aggregation. We hypothesized that oligomerization of PABPN1 facilitates OPMD intranuclear protein aggregation. Here we report that oligomerization of PABPN1 is mediated by two potential oligomerization domains (ODs). Deletion of 6–8 amino acids in either of the ODs inactivates oligomerization of mPABPN1 and prevents protein aggregation. In addition, we showed that expression of mPABPN1 in COS-7 cells is associated with cell death, and that preventing protein aggregation by deletions in the ODs can significantly reduce cell death.

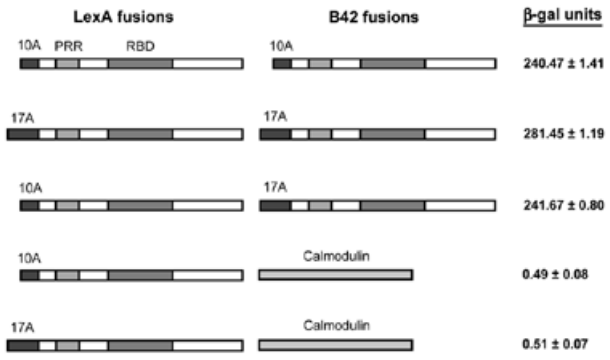

Figure 1. Yeast two-hybrid analysis of PABPN1 self-association. The wild-type PABPN1 (wtPABPN1) and the mutated PABPN1 (mPABPN1) were fused to the LexA DNA binding domain, and also fused to the B42 transcription activation domain. The LexA fusion proteins were co-expressed in yeast with B42 fusion proteins. The *LacZ* gene was used as a reporter gene. The interaction between two co-expressed proteins in yeast was characterized as positive if the yeast cells express β-galactosidase. The truncated calmodulin was used as a negative control. β-Gal units were obtained by measuring the β-galactosidase activity in the yeast cell co-expressing the left two proteins using a liquid assay (mean ± SD). 10A, 10-alanine stretch in the wtPABPN1; 17A, 17-alanine stretch in the mPABPN1; PRR, proline-rich region; RBD, putative RNA binding domain.

RESULTS

PABPN1 self-association

PABPN1 forms both linear filaments and discrete-sized, compact oligomeric particles in the presence of mRNA (37), and oligomers in the absence of mRNA (38). However, it is not known how PABPN1 molecules interact with each other. We tested the interaction between two wild-type PABPN1 with 10 alanines (wtPABPN1), two mutated PABPN1 with 17 alanines (mPABPN1), and wtPABPN1 and mPABPN1, using the yeast two-hybrid assay. We observed strong interactions using all these combinations (Fig. 1), suggesting that alanine expansion in this protein does not affect the capacity to form strong self-association. The RNA binding activity of PABPN1 could lead to false positives in the yeast two-hybrid assay, since two testing molecules can be bridged together by poly(A) tails. In order to confirm the self-association of PABPN1, a glutathione *S*-transferase (GST) pull-down assay was applied. GST–wtPABPN1, not GST alone, is able to pull-down HA–wtPABPN1, indicating that self-association of PABPN1 can be detected *in vitro* (Fig. 3C).

Mapping the potential PABPN1 ODs

In order to map the ODs, we generated a series of truncated PABPN1 proteins and examined the interaction among these truncated proteins using the yeast two-hybrid assay (Fig. 2). We observed that the C-terminus of PABPN1 (249–306) without the putative RNA binding domain is able to interact with wtPABPN1, indicating that a potential OD resides in its C-terminus (Fig. 2A). Narrowing down the region in the C-terminus, the potential domain was revealed to lie between amino acids 264 and 306, $OD_{(264–306)}$. Deletion of five

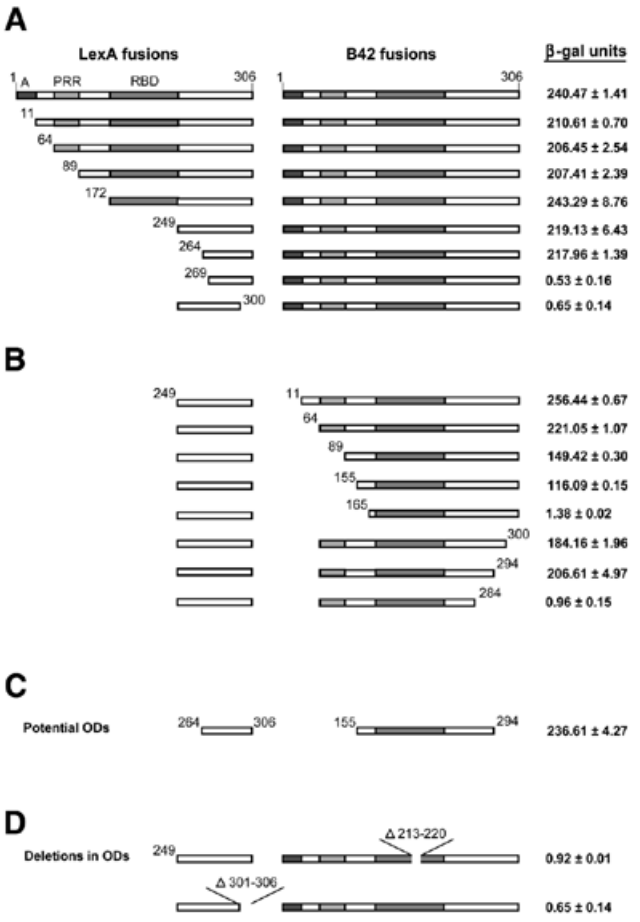

Figure 2. Mapping the ODs in PABPN1 and inactivating oligomerization by deletion mutagenesis. A series of PABPN1 truncated proteins was generated as detailed in Materials and Methods. The protein–protein interactions of all the combinations were detected using the yeast two-hybrid assay as described in Figure 1. (**A**) The N-terminal boundary of the potential oligomerization domain $OD_{(264–306)}$ was identified by truncating PABPN1 from the N- to C-terminus and examining the interactions between these truncated proteins and wtPABPN1. A switch from positive to negative interaction was used as a marker for identifying the boundary of the OD. The C-terminal boundary of $OD_{(264–306)}$ was determined by truncating the protein from the C- to the N-terminus. (**B**) The same method was used to identify the boundaries of $OD_{(155–294)}$ with the exception that the interaction was examined between the various truncated proteins and only the C-terminus of PABPN1, which contains $OD_{(264–306)}$. (**C**) Two potential ODs interact with each other. (**D**) The deletions (Δ301–306) in $OD_{(264–306)}$ and (Δ213–220) in $OD_{(155–294)}$ were found to inactivate the interaction between two ODs.

additional residues (264–268) from the N-terminus or six residues (301–306) from the C-terminus inactivated the interaction (Fig. 2A). We next tested the interaction between the PABPN1 C-terminus (249–306) and the other truncated proteins, and identified another potential OD that resides within the segment from amino acids 155 to 294, $OD_{(155–294)}$ (Fig. 2B). Deletion of 10 additional residues (155–164) from the N-terminus or (285–294) from the C-terminus abolished the interaction (Fig. 2B). These two potential ODs interacted with each other (Fig. 2C). Interestingly, the ODs overlap and are located in the C-terminus from amino acids 155 to 306, far from the polyalanine stretch in the N-terminus. Thus, we suggest that oligomerization of PABPN1 is probably mediated by these two potential ODs.

Inactivating oligomerization of PABPN1 by deletions in the ODs

To determine whether oligomerization of PABPN1 plays a role in the formation of the intranuclear protein aggregation in OPMD, we made a series of deletions to inactivate both ODs. Among these deletions, either removal of eight amino acids (Δ213–220) in $OD_{(155–294)}$ or six residues (Δ301–306) in $OD_{(264–306)}$ effectively inactivates self-association of PABPN1 detected by the yeast two-hybrid assay (Fig. 2D) and GST pull-down assay (Fig. 3). GST–wtPABPN1 is able to pull-down either of the two OD mutants. PABPN1 with a deletion in one OD can pull-down the PABPN1 with a deletion in the other OD, but cannot pull-down the protein with a deletion in the same OD.

Intranuclear aggregates induced by over-expression of mPABPN1 in COS-7 cells are insoluble

Two groups previously reported that over-expression of mPABPN1 results in formation of large intranuclear protein aggregates. Our group reported that over-expression of mPABPN1 in COS-7 cells results in the formation of intranuclear protein aggregation 3 days after transfection (42). Another group more recently reported that HeLa cells over-expressing mPABPN1 also show large intranuclear aggregate bodies 2 days after transfection (43). The PABPN1 present in the intranuclear inclusions from OPMD patients is insoluble and resistant to KCl treatment that is known to be able to dissolve soluble protein aggregates (39). In order to determine whether the intranuclear aggregates induced by mPABPN1 in our OPMD cellular model are also insoluble, we expressed green fluorescent protein (GFP)-tagged wtPABPN1 and GFP–mPABPN1 in COS-7 cells. In 3 days the transfected cells were either fixed or treated with KCl before fixation to dissolve the soluble proteins. The microtome sections of the deltoid muscle from a control subject and an OPMD patient were also either immunostained using anti-PABPN1 antibody or treated with KCl before immunostaining. As previously reported, the PABPN1 present in the nuclear inclusions from the OPMD patient is insoluble and resistant to KCl treatment, while the one present in the muscle nuclei from the control subject is soluble and dissolved in KCl (Fig. 4). The aggregates induced by GFP–mPABPN1 are also insoluble and remained after KCl treatment, whereas the GFP–wtPABPN1 signal is soluble and not resistant to KCl treatment (Fig. 4). Thus, the aggregates induced by mPABPN1 in COS-7 cells and the nuclear inclusions in OPMD patients share the same insoluble property of resistance to KCl treatment.

Inactivating oligomerization of mPABPN1 prevents protein aggregation

To investigate whether oligomerization of PABPN1 plays a role in the formation of OPMD intranuclear protein aggregation, the proteins wtPABPN1, mPABPN1, mPABPN1 (Δ213–220) and mPABPN1 (Δ301–306) were fused to GFP (Fig. 5A), and expressed in COS-7 cells. Unlike GFP, which localizes to the cytoplasm and nucleus,

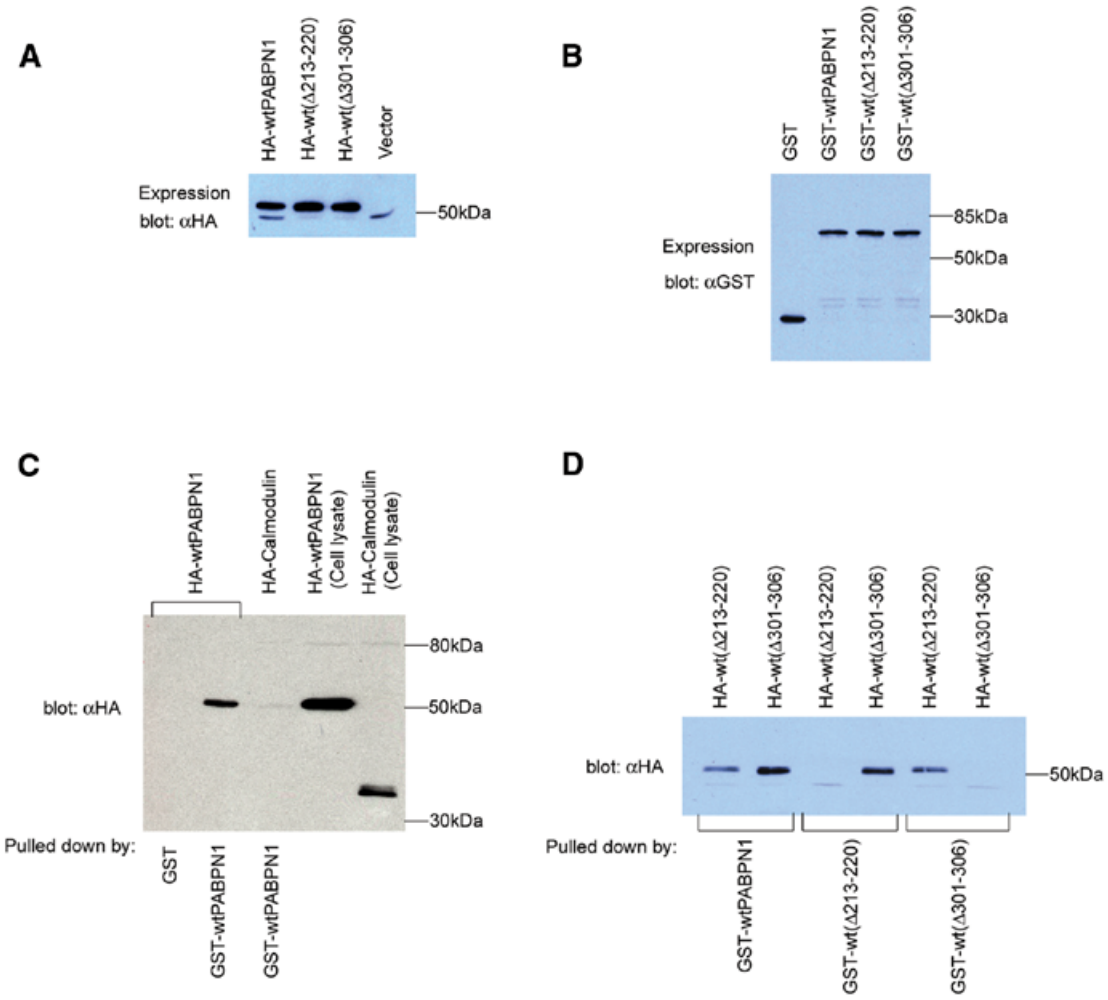

Figure 3. GST pull-down analysis of the interaction between wtPABPN1 and its deletion mutants. (**A**) Expression of HA–wtPABPN1, HA–wtPABPN1 (Δ213–220) and HA–wtPABPN1 (Δ301–306). The HA-tagged proteins were expressed in yeast, extracted and resolved on SDS–PAGE and detected using an antibody against the HA epitope. (**B**) Expression of GST, GST–wtPABPN1, GST–wtPABPN1 (Δ213–220) and GST–wtPABPN1 (Δ301–306). The proteins were expressed in bacteria, purified and detected using the anti-GST polyclonal antibody. (**C**) PABPN1–PABPN1 interaction detected using GST pull-down assay. HA–wtPABPN1 was incubated with 5 µg of GST or GST–wtPABPN1, pulled-down by glutathione Sepharose 4B beads and assayed by western blotting using the anti-HA polyclonal antibody. The HA-tagged truncated Calmodulin protein was used as a negative control. Two lanes on the right side are cell lysates to show the sizes of HA-tagged proteins. (**D**) Deletions in the ODs of wtPABPN1 inactivate the PABPN1–PABPN1 interaction. HA–wtPABPN1, HA–wtPABPN1 (Δ213–220) and HA–PABPN1 (Δ301–306) were incubated with 5 µg of GST fusion proteins, and pulled-down and assayed using the same strategy as described in (C).

wtPABPN1 is predominantly localized to the nucleus. Cells expressing GFP–wtPABPN1 show a strong GFP signal in the nuclei (Fig. 5B). Like wtPABPN1, mPABPN1 is predominantly localized to the nucleus, but appears in a form of protein aggregates in most nuclei of transfected cells (Fig. 5B). Western blotting analysis showed that some GFP–mPABPN1 prepared from the COS-7 cells on day 3 after transfection can be detected as aggregates at the top of the stacking gel while only a small portion of wtPABPN1 is present in this insoluble fraction (Fig. 5C). These observations suggest that mPABPN1 is sufficient to induce the formation of intranuclear protein aggregation. The deletion (Δ213–220) or (Δ301–306) in mPABPN1 abolishes protein aggregation in cells and insoluble fraction in the stacking gel of SDS–PAGE (Fig. 5B and C). These observations suggest that inactivating oligomerization by deletions in the ODs can prevent protein aggregation induced by the expansion of the polyalanine stretch of PABPN1. We also observed that insoluble GFP–mPABPN1 is barely detected on day 1, 2 or 4 in the stacking gel, and GFP–mPABPN1 with 13 alanines is hard to detect at any time points after transfection (data not shown).

Nuclear protein aggregation is associated with cell death

We expressed GFP-tagged wtPABPN1, mPABPN1 and non-oligomerizing forms of mPABPN1 in COS-7 cells and counted the number of transfected cells every 24 h after transfection. The cells expressing GFP or GFP–wtPABPN1 gradually die within 8 days after transfection (Fig. 6B). However, the ones expressing GFP–mPABPN1 die more rapidly, with >50% of the cells dying within the first 4 days (Fig. 6). The percentage of living cells transfected with GFP–mPABPN1 is significantly

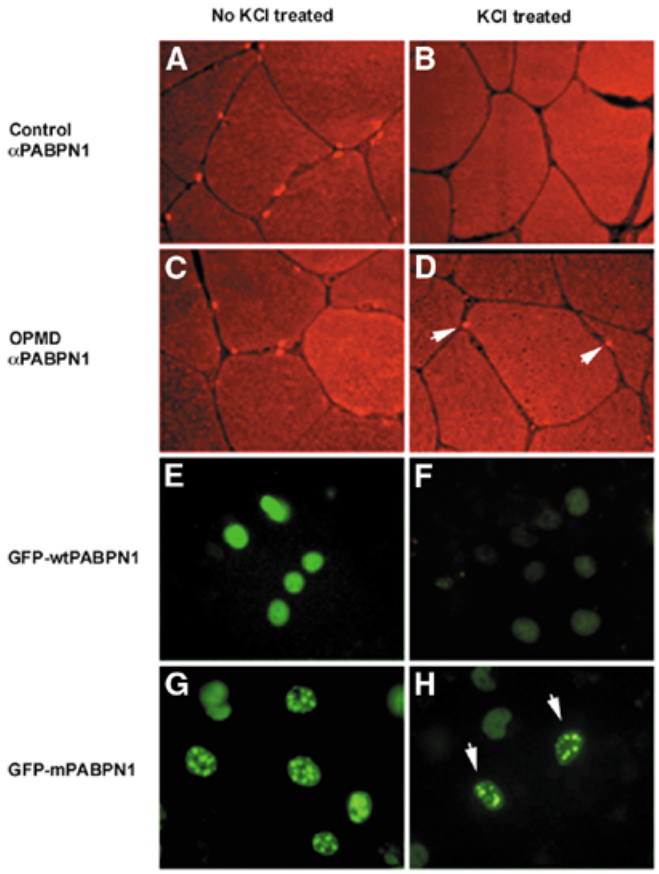

Figure 4. Expression of mPABPN1 induces insoluble intranuclear aggregates. Immunohistochemistry (**A**–**D**): the cross microtome sections of the deltoid muscle from a control subject (A and B) and an OPMD patient (C and D) were either immunostained using anti-PABPN1 antibody (A and C) or treated with 1 M KCl in HPEM buffer for 5 min at room temperature before being immunostained to dissolve the soluble proteins (B and D). Arrowheads indicate the positively stained insoluble intranuclear inclusions. Cytochemistry (**E**–**H**): GFP–wtPABPN1 (E and F) and GFP–mPABPN1 (G and H) were transiently expressed in COS-7 cells. Three days after transfection, the cells were either fixed (E and G) or treated with KCl before fixation (F and H). Arrowheads indicate the nuclei containing insoluble aggregates induced by expression of GFP–mPABPN1.

lower compared with cells expressing GFP or GFP–wtPABPN1 on days 4, 5, 6 and 7. Interestingly, the percentages of living cells expressing GFP–mPABPN1 (Δ213–220) or GFP–mPABPN1 (Δ301–306) are not significantly different from those expressing GFP or GFP–wtPABPN1 at any time point examined (Fig. 6). We therefore conclude that mPABPN1 expression is associated with cell death and that preventing mPABPN1-induced protein aggregation is able to reduce cell death.

DISCUSSION

OPMD is caused by expansion of a polyalanine stretch in PABPN1 from 10 residues to 12–17 residues (12), which leads to intranuclear protein aggregation and cellular toxicity (42). In addition to the genetic evidence, PABPN1 is detected in OPMD nuclear inclusions by immunohistochemistry (39,40), indicating that this protein plays a direct role in intranuclear protein aggregation. It has been shown that expression of an alanine stretch of more than 19 residues alone is able to form aggregates in cells and cause cell death (44). The alanine stretches in the wild-type transcription factors HOXD13, HOXA13, FOXL2, CBFA1 and ZIC2 range from 14 to 17 alanines, and do not result in protein aggregation (13–17). The fact that the relatively small 12-alanine stretch in PABPN1 induces protein aggregation and causes dominant OPMD symptoms (12) suggests that there must be other characteristics of PABPN1 than the alanine stretch that promote or facilitate nuclear protein aggregation and cause toxicity. It has been shown that PABPN1, when bound to the poly(A) tail of mRNA, forms both linear filaments and discrete-sized, compact oligomeric particles *in vitro* (37), and can form oligomers in the absence of mRNA (38). These observations led us to predict that oligomerization of PABPN1 contributes to the formation of OPMD intranuclear protein aggregation and toxicity, and that inactivating oligomerization may prevent these phenotypes. The observations described here provide two lines of evidence to support this hypothesis. First, the expanded alanine stretch itself is necessary but not sufficient to induce nuclear protein aggregation in our OPMD cellular model; secondly, oligomerization of mPABPN1 facilitates the formation of protein aggregation, while inactivating oligomerization by deletions in the ODs can prevent protein aggregation.

Two potential ODs of PABPN1, $OD_{(155–294)}$ and $OD_{(264–306)}$, were mapped out using the yeast two-hybrid assay. Mutations in either of these domains abolished the self-association. This assay is an efficient and sensitive method to study protein–protein interactions. But when testing the interaction between RNA binding proteins, false positive results may occur since RNA can bridge two testing proteins together. The self-association of PABPN1 was confirmed by GST pull-down assay, suggesting that PABPN1 self-association is a true positive caused by protein–protein interaction rather than by RNA binding. In addition, $OD_{(264–306)}$ is located at the end of the protein outside the putative RNA binding domain, suggesting that the interaction between two ODs is not a false positive caused by RNA binding. These two ODs overlap one another, suggesting that this protein could not perform intra-molecular interactions and form a 'closed' conformation. Both of the ODs are located near the C-terminus of PABPN1 (among amino acids 155–306), far from the polyalanine stretch amino acids 2–11. Deletion of the N-terminus from amino acids 1 to 154 does not affect oligomerization (Fig. 2), indicating that the N-terminus has a very weak effect on oligomerization. This might explain why polyalanine expansion in the N-terminus does not affect its oligomerization.

PABPN1 is an abundant nuclear protein that has been localized to clusters of interchromatin granules and visualized as speckles in the nuclei of HeLa cells by immunocytochemistry (45,46). We did not observe speckles in the majority of cells expressing wtPABPN1, most likely because of over-expression; the overwhelming fluorescent signal in the nucleus could mask the interchromatin granule speckles. Over-expression of mPABPN1 leads to the formation of large insoluble aggregates in most nuclei of transfected COS-7 cells. These insoluble aggregates are best detected in the SDS–PAGE stacking gel on day 3 after transfection, since >60% of the transfected cells are dead on day 4 or later time points (Fig. 6B). We speculate that

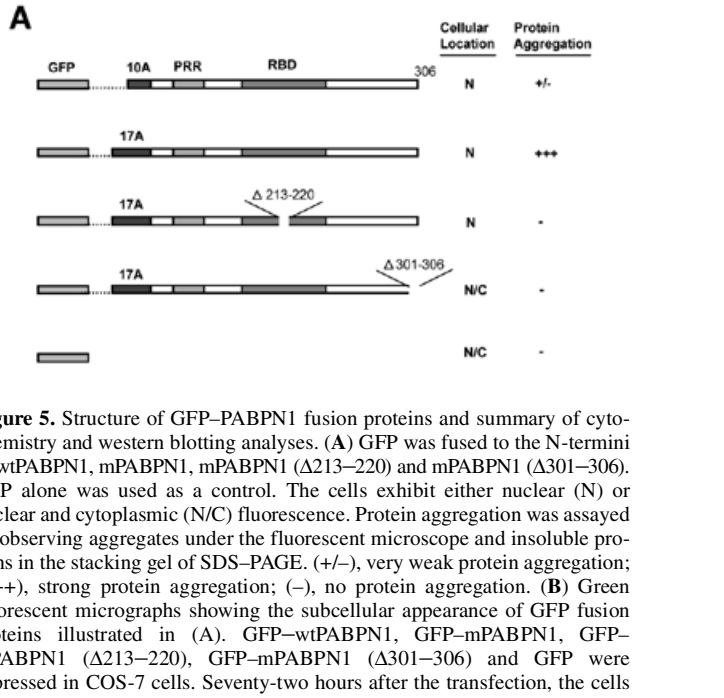

Figure 5. Structure of GFP–PABPN1 fusion proteins and summary of cytochemistry and western blotting analyses. (**A**) GFP was fused to the N-termini of wtPABPN1, mPABPN1, mPABPN1 (Δ213–220) and mPABPN1 (Δ301–306). GFP alone was used as a control. The cells exhibit either nuclear (N) or nuclear and cytoplasmic (N/C) fluorescence. Protein aggregation was assayed by observing aggregates under the fluorescent microscope and insoluble proteins in the stacking gel of SDS–PAGE. (+/–), very weak protein aggregation; (+++), strong protein aggregation; (–), no protein aggregation. (**B**) Green fluorescent micrographs showing the subcellular appearance of GFP fusion proteins illustrated in (A). GFP–wtPABPN1, GFP–mPABPN1, GFP–mPABPN1 (Δ213–220), GFP–mPABPN1 (Δ301–306) and GFP were expressed in COS-7 cells. Seventy-two hours after the transfection, the cells were fixed and visualized under the fluorescence microscope. (**C**) Western blotting analysis of GFP fusion proteins illustrated in (A). COS-7 cells expressing GFP, GFP–wtPABPN1, GFP–mPABPN1, GFP–mPABPN1 (Δ213–220) and GFP–mPABPN1 (Δ301–306) were lysed 3 days after transfection. The lysates were resolved on SDS–PAGE. GFP fusion proteins were detected using monoclonal antibody against GFP epitope.

it may take at least 2 days for the transfected cells to form insoluble aggregates, since the insoluble aggregates are barely detected on day 1 and 2 in the western stacking gel. The length of the expanded polyalanine might affect the formation of insoluble aggregates. The insoluble aggregates induced by mPABPN1 with 13 alanines are hard to detect in the stacking gel, while the ones induced by mPABPN1 with 17 alanines are relatively easy to see. Therefore, we believe that the longer the polyalanine stretch is, the more insoluble aggregates are formed. As is seen in OPMD patients, the intranuclear aggregates induced by expression of mPABPN1 in COS-7 cells are insoluble and resistant to KCl treatment. Electron microscope studies showed that mPABPN1-induced aggregates are morphologically similar to the intranuclear inclusions from OPMD patients (H.Lavoie and B.Brais, manuscript in preparation). These observations imply that mPABPN1 is able to induce insoluble nuclear protein aggregation in cells in as short a period of time as 3 days post-transfection, and that expressing mPABPN1 in COS-7 cells as an OPMD cellular model for pathological study is a suitable tool.

We hypothesized that oligomerization and poly(A) binding activity of mPABPN1 facilitate the formation of OPMD intranuclear protein aggregation. The deletion of six residues from amino acids 301 to 306 inactivates the oligomerization of PABPN1, but it should not affect the RNA binding activity since it has been shown that deletion of eight amino acids from 299 to 306 does not affect its RNA binding activity of PABPN1 (U.Kuhn and E.Wahle, personal communication). The polyalanine expanded PABPN1 bearing deletion of amino acids 301–306 does not induce protein aggregation, suggesting that RNA binding activity of mPABPN1 alone is not sufficient to facilitate protein aggregation. We have recently identified a nuclear localization signal (NLS) that resides at the C-terminus of PABPN1 from amino acids 289–306, and deletion of amino acids 301–306 inactivates the function of the NLS (unpub-

lished data). However, mPABPN1 bearing this deletion is still able to enter the nucleus, possibly by diffusion due to its small molecular weight, but does not aggregate. These observations suggest that inactivating the oligomerization of mPABPN1 could prevent protein aggregation in both the nucleus and the cytoplasm. In SCA1, nuclear localization of the polyglutamine expanded ataxin-1 protein is critical to initiate pathogenesis; transgenic mice carrying polyglutamine expanded ataxin-1 with a mutated NLS do not develop disease (52). In order to understand whether nuclear localization of mPABPN1 is necessary to initiate OPMD pathogenesis, we are currently trying to exclude mPABPN1 from the nucleus by fusing a nuclear export sequence to mPABPN1 and examining the toxicity in our OPMD cellular model, as well as transgenic mice. The deletion from amino acids 213 to 220 in $OD_{(155–294)}$ can also inactivate the oligomerization. The mPABPN1 bearing this deletion is still able to localize to the nucleus but does not form protein aggregates (Fig. 5B). This deletion is in the middle of the putative RNA binding domain, and may affect its RNA binding activity. Because the RNA binding has a weak effect on protein aggregation, we believe that inhibition of protein aggregation by deletion of amino acids 213–220 is mainly caused by inactivation of oligomerization, rather than abolishing its RNA binding activity. Thus, we conclude that oligomerization of mPABPN1 facilitates the formation of OPMD protein aggregation, while the expanded alanine stretch in PABPN1 is necessary but not sufficient for the formation of this type of protein aggregation.

The presence of abnormal protein aggregates is a relatively common finding in a number of neuronal degenerative diseases (47,48). The best characterized and most common of such disorders is HD, which results from an expansion of the polyglutamine stretch in huntingtin, leading to its aggregation and abnormal association with various cell proteins (49). Eventually, impaired neuronal function becomes evident and may trigger cell death (50). It has been widely assumed that aggregate formation is a critical event triggering neuropathology in this disease (48). However, there is also appreciable evidence against this view. Deletion of the C-terminal portion of huntingtin enhances the formation of inclusions but does not increase the fraction of apoptotic cells (51). Furthermore, in SCA1, deletion of the self-association regions of ataxin-1 blocks aggregation but does not suppress apoptosis (52). In order to identify whether OPMD protein aggregation is associated with cell death, we expressed the full-length mPABPN1, wtPABPN1 and non-oligomerizing forms of mPABPN1 in COS-7 cells, and examined cell survival at different time points after transfection. We found that OPMD protein aggregation is associated with accelerated cell death. Blocking mPABPN1-induced protein aggregation can reduce cell death, suggesting that mPABPN1-induced protein aggregation is a critical event in the pathophysiology of OPMD. In another study we have looked for apoptosis in cells expressing mPABPN1, and found that apoptotic caspases 1, 6, 8 and 9 are not activated, apoptosis staining (TUNEL) is insignificant, PARP protein cleavage is not detectable and apoptotic morphology cannot be observed (H. Lavoie and B. Brais, manuscript in preparation). Therefore, we believe that cell death in OPMD may be caused by a non-apoptotic mechanism as reported in a cellular model of SCA3 and a transgenic model of HD (53,54).

It has been initially assumed that subcellular inclusions result from the inherent tendency of misfolded proteins to associate with one another to form insoluble aggregates. Recent findings indicate that inclusion formation in mammalian cells is a more complex, multi-step process, in which cellular machinery appears to be actively involved (55–57). Unlike the neurodegenerative diseases that are associated with expansions of polyglutamine stretches in the mutated proteins, OPMD is caused by a short expansion of polyalanine stretch in PABPN1. The polyalanine stretch expansion from 10 to 12 is sufficient to cause dominant OPMD disorder, while some wild-type transcription factors contain a non-pathological stretch of around 15 alanines. Therefore, it is likely that the toxicity of this short polyalanine stretch is partly dependent on the host protein. In PABPN1, the other parts of the protein most likely play a role in OPMD toxicity. OPMD intranuclear inclusions were reported to sequester poly(A) RNA and suggested to interfere with the poly(A) RNA export from the nucleus to cytoplasm (39). Here we propose a model to explain the molecular mechanism for the OPMD phenotypes. Expansion of polyalanine stretch in PABPN1 causes misfolding and exposes its hydrophobic alanine stretch that would otherwise be buried inside in the wild-type form. The longer the polyalanine stretch is, the more exposed the hydrophobic region is. Misfolded mPABPN1 therefore acquires a gain of function and is able to perform weak self-association through the exposed hydrophobic regions. Because the polyalanine stretch is located at the N-terminus, far from both ODs, the expanded polyalanine stretch does not interfere with the oligomerization. When the mPABPN1 performs weak self-association through the hydrophobic regions, oligomerization of mPABPN1 facilitates this weak self-association by linking mPABPN1 molecules together and leads to inclusion formation. Concurrently, mPABPN1 is detected and bound by chaperones, components of the ubiquitin–proteasome pathway, as well as other crucial proteins. Binding of these proteins to mPABPN1 may promote refolding, solubilization and/or degradation of mPABPN1. Essentially, there is a balance between mPABPN1 elimination and aggregation. Upon aging of the cell, its ability to deal with abnormal proteins may decrease, therefore resulting in a tilt in balance favoring protein aggregation. Because PABPN1 coats the poly(A) tail of mRNA in the nucleus, the OPMD intranuclear protein aggregates may sequester mRNA and interfere with mRNA export. Interfering with mRNA export is detrimental to cells and causes cell death. Inactivating the oligomerization of mPABPN1 slows the formation of aggregates and allows the ubiquitin–proteasome pathway to degrade the mutated proteins more efficiently, therefore preventing the formation of protein aggregation.

Inactivating oligomerization of mPABPN1 prevents protein aggregation and reduces cell death in our OPMD cellular model, suggesting that the ODs may be useful therapeutic targets for OPMD. Identification and testing of compounds or peptides that inactivate oligomerization of mPABPN1 would further confirm our findings.

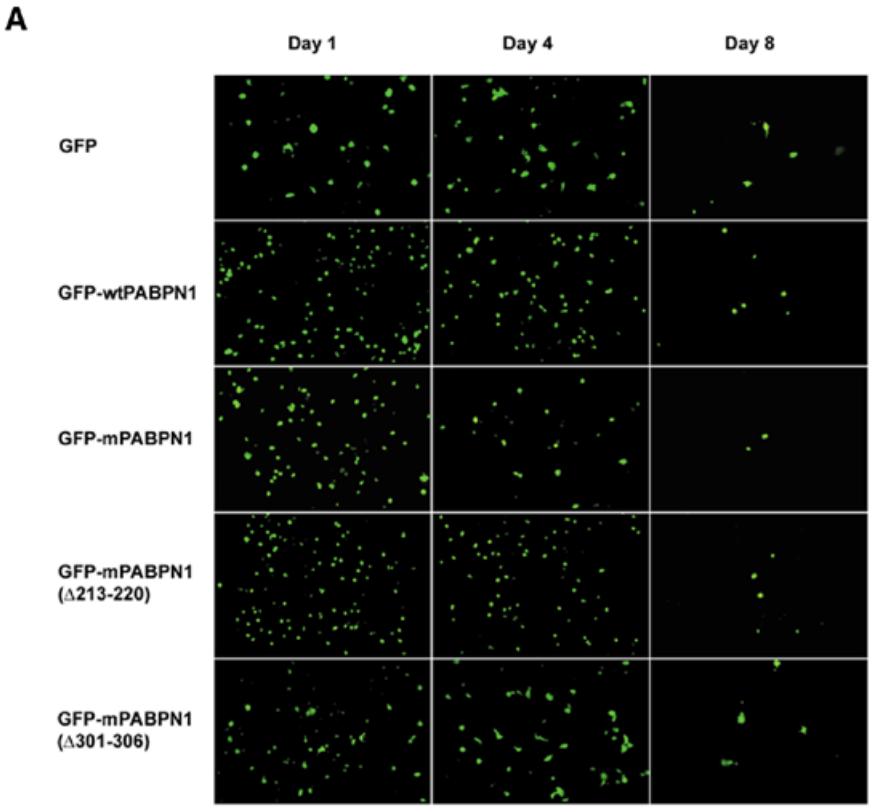
A
Day 1
Day 4
Day 8
GFP
GFP-wtPABPN1
GFP-mPABPN1
GFP-mPABPN1 (Δ213-220)
GFP-mPABPN1 (Δ301-306)

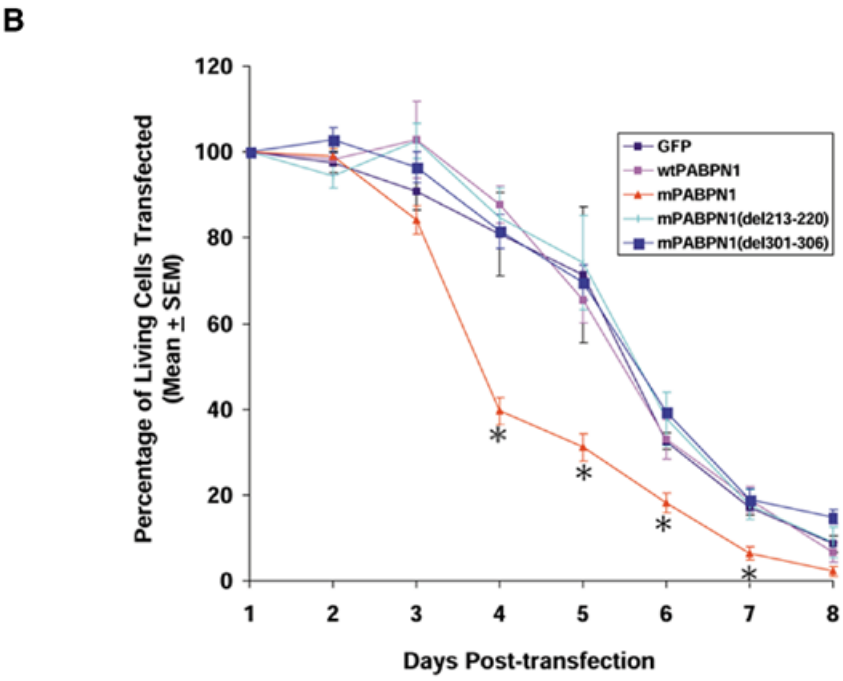
B
Percentage of Living Cells Transfected (Mean ± SEM)
Days Post-transfection
GFP
wtPABPN1
mPABPN1
mPABPN1(del213-220)
mPABPN1(del301-306)
120
100
80
60
40
20
0
1
2
3
4
5
6
7
8
*

MATERIALS AND METHODS

Yeast two-hybrid assay

The DupLEX-A™ yeast two-hybrid system (OriGene Tech, Rockville, MD) was used to detect the PABPN1–PABPN1 interaction and map out the ODs. The constructs were made by amplifying required regions of the cDNA using *Pfu* DNA polymerase (Stratagene, La Jolla, CA). Primers 5′-P64 (CTG GAA TTC GCC GAG CCG GAG CCC GAG CCC GAA G), 5′-P89 (CCT GAA TTC GGT TCG GGA GCC CCC GGC AGC CAA G), 5′-P155 (CCT GAA TTC AAT GCT GGC CCG GTG ATC ATG TCC), 5′-P165 (TCC GAA TTC GAG AAG ATG GAG GCT GAT GCC CGT TC), 5′-P172 (GCT GAA TTC CGT TCC ATC TAT GTT GGC AAT GTG), 5′-P249 (CA GAA TTC ACC AAC AGA CCA GGC ATC AGC ACA AC), 5′-P264 (TTT GAA TTC GCC CGC TAC CGC GCC CGG ACC ACC) and 5′-P269 (TAC GAA TTC CGG ACC ACC ACC TAC AAC AGC TCC) were used in conjunction with 3′-PABPN1 (TT GGA TCC TCT CTC TCC TCC TAA TAC ACA CTT) to generate truncated forms of PABPN1 (64–306), (89–306), (155–306), (165–306), (172–306), (249–306), (264–306) and (269–306), respectively. The truncated protein (11–306) was generated by restriction digestion of the full-length PABPN1 cDNA using *Msp A1*. The cDNAs encoding peptide (249–300) was amplified using 5′-P249 in conjunction with 3′-P300 (GGA GGA TCC TCA TGT CGC TCT AGC CCG GCC CCT GTA GAC). Peptides (89–300), (89–294) and (89–284) were generated using primers 5′-P89 in conjunction with 3′-P300, 3′-P294 (TCT GGA TCC TCA CCT GTA GAC GCG ACC CCG GGG CCT GC) and 3′-P284 (GGG GGA TCC TTA AAA ACC ACT GTA GAA TCG AGA GC), respectively. Amplified DNA products were digested with *Eco*RI–*Bam*HI, and cloned into vector pEG202NLS, which allowed PABPN1 and its truncated proteins to be fused to the LexA DNA binding domain and an NLS. The cDNAs encoding PABPN1 and its truncated proteins (11–306), (64–306), (89–306), (155–306), (165–306), (89–300), (89–294) and (89–284) were released by cutting the constructs with *Eco*RI–*Sal*I and cloned into pJG4-5 vector to fuse the PABPN1 truncated proteins to the B42 transcription activation domain and HA epitope tag. All constructs were verified by DNA sequencing. The *LacZ* gene in the construct pSH18-34 was used as a reporter gene. The constructs pEG202NLS-PABPN1 (or its deletions), pJG4-5-PABPN1 (or its deletions) and pSH18-34 were co-transformed into *EGY48* yeast cells. The interaction between the two co-expressed proteins in yeast was characterized as positive if yeast cells expressed β-galactosidase. Protein expression was confirmed by western blotting using polyclonal antibodies against LexA (Santa Cruz Biotech, CA) and HA epitope (Santa Cruz Biotech).

β-galactosidase liquid assays

The yeast cells expressing the proteins being tested are grown in supplemented YNB(Gal/Raf) medium at 30°C. At mid-log growth (A_{600} ~0.6), A_{600} of the cells is measured, and 1 ml of yeast in medium is transferred to an Eppendorf (in triplicate), washed with Z buffer (60 mM Na_2HPO_4, 40 mM NaH_2PO_4, 10 mM KCl, 1 mM $MnSO_4$). The yeast cells are pelleted and suspended in 150 µl of Z buffer with 50 mM β-mercapto-ethanol (BME), and added with 50 µl of chloroform, 20 µl of 10% SDS. The tube was vortexed for 15 s, 700 µl of ONPG (1 mg/ml in Z buffer with BME) added, and incubated at 30°C. The incubation time was measured. An aliquot of 0.5 ml of 1 M Na_2CO_3 was added to stop the reaction when the solution turned yellow. The supernatant was used to measure the OD at A_{420}. The β-galactosidase unit was calculated using the formula $[A_{420} \times 1000]/A_{600} \times$ time (in min) $\times$ volume (in ml).

Site-directed mutagenesis

The QuikChange™ Site-Directed Mutagenesis Kit (Stratagene, La Jolla, CA) was used to generate the desired deletions in the various PABPN1 constructs. All procedures were performed according to the manufacturer's instructions. The deletions were confirmed by DNA sequencing. For deletion of amino acids 213–220, primer 5′-Δ213–220 (CTG TGT GAC AAA TTT AGT GGC CAT CCC TCA GAC AAA GAG TCA GTG AGG ACT TCC) in conjunction with 3′-Δ213–220 (GGA AGT CCT CAC TGA CTC TTT GTC TGA GGG ATG GCC ACT AAA TTT GTC ACA CAG) was used to generate the desired deletion.

In vitro binding assay

To generate GST fusion proteins, the cDNA fragments for PABPN1, PABPN1(Δ213–220) and PABPN1(Δ301–306) were cut out from the pEG202NLS constructs using *Eco*RI–*Sal*I, and cloned into the GST vector pGEX-5X-1 (Amersham Pharmacia Biotech, Piscataway, NJ), which allowed the fusion of GST to the N-termini of PABPN1 proteins. Constructs were verified by DNA sequencing, and transformed into *Escherichia coli XL1-Blue*. The Bulk and RediPack GST purification modules (Amersham Pharmacia Biotech) were used for expression and purification of GST fusion proteins according to manufacturer's instructions. Purified fusion proteins were confirmed by western blotting using anti-GST antibody. PABPN1 cDNAs cut out by *Eco*RI–*Sal*I from pEG202NLS constructs were also subcloned into yeast vector pJG4-6, which allowed PABPN1, PABPN1(Δ213–220) and PABPN1(Δ301–306) to be fused to the HA epitope. All constructs were verified by DNA sequencing. The HA-tagged proteins were expressed in the yeast strain EGY48 and confirmed by western blotting using the antibody against HA epitope. The yeast cells expressing HA-tagged PABPN1

Figure 6. (**A**) Green fluorescent micrographs showing the density of the living cells expressing GFP–PABPN1 fusion proteins on days 1, 4 and 8 after transfection. The COS-7 cells expressing GFP fusion proteins illustrated in Figure 5A were fixed and visualized under a fluorescence microscope on days 1, 4 and 8 after transfection. The micrographs were taken under a low magnification (30×) to show the density of the living transfected cells. The density of living cells expressing mPABPN1 is dramatically decreased on day 4 compared with day 1. (**B**) Percentage of living cells expressing GFP–PABPN1 fusion proteins at different times post-transfection. The cells were counted every 24 h post-transfection. Each well was counted three times in different areas at one time point, and the mean was used for statistics. The percentage of living cells transfected represents the variation of the amount of living transfected cells at different time points compared with the number of transfected cells obtained on day 1. Mean ± SEM; $n = 6$; $^*P < 0.05$ compared with any other groups (ANOVA analysis).

proteins were lysed by vortexing with glass beads. The lysates were incubated overnight at 4°C with a 5 µg GST fusion protein and glutathione Sepharose 4B beads. The beads were washed four times with lysis buffer, suspended in 40 µl of protein sample buffer and heated to 95°C for 5 min. GST pulled-down proteins were resolved on 12% SDS–PAGE gel and blotted with polyclonal anti-HA antibody.

Cell culture and transfection

The cDNAs encoding wtPABPN1, mPABPN1 (with 17 alanines, as seen in OPMD patients), mPABPN1 (Δ213–220) and mPABPN1 (Δ301–306) were cloned into pEGFP-C2 vector (Clontech, Palo Alto, CA), resulting in a fusion of GFP to the N-termini of PABPN1 proteins. The day before transfection, COS-7 cells were seeded in Dulbecco's modified Eagle's medium (DMEM) (Gibco BRL, MD) containing 10% fetal calf serum (Gibco BRL) at a concentration of 2×10^5 cells per well in six-well plates containing sterile coverslips. COS-7 cells were transfected with plasmid DNA (2.0 µg) using Lipofectamine reagent (Gibco BRL) according to the manufacturer's instructions. The cells were fixed after 72 h with 4% paraformaldehyde and then visualized using a fluorescence microscope with a filter appropriate for GFP in three independent experiments. To remove the soluble proteins, the cells expressing GFP–wtPABPN1 and GFP–mPABPN1 were treated with 0.5 M KCl in HPEM (30 mM HEPES, 65 mM PIPES, 10 mM EDTA, 2 mM $MgCl_2$, pH 6.9) for 5 min at room temperature before fixation. The number of living cells was measured every 24 h post-transfection. Briefly, each well was washed with DMEM to remove detached cells and the cells expressing GFP were counted in 1 mm^2 area under low magnification (30×). Three different areas were counted for each well. All wells were in duplicate and the experiment was repeated three times ($n = 6$).

Immunohistochemistry

The microtome sections of paraffin-embedded deltoid muscle from an OPMD patient and a control subject were used. Sections were deparaffinized, permeabilized and immunostained using polyclonal anti-PABPN1 antibody and rhodamine-conjugated secondary antibody. The signal was visualized using a fluorescence microscope with an appropriate filter for rhodamine. To remove the soluble proteins, the deparaffinized sections were treated with 1 M KCl in HPEM for 5 min at room temperature before the immunostaining was performed.

Western blotting

Seventy-two hours after transfection the COS-7 cells expressing GFP–PABPN1 fusion proteins were harvested. The proteins were separated using 12% SDS–PAGE and transferred to a nitrocellulose membrane. The membrane was probed with a monoclonal anti-GFP antibody (Clontech) (1:2000), and detected using the Western Blot Chemiluminescence Reagent *Plus* kit (NEN Life Science Products, Boston, MA).

ACKNOWLEDGEMENTS

We are very grateful to Uwe Kuhn and Dr Elmer Wahle for sharing information, and to Dr Mehrdad Jannatipour for demonstrating useful technical help and comments. We are grateful to Daniel Rochefort for his invaluable suggestions on construct making. We thank Dr Claudia Gaspar and Dr Andre Toulouse for careful reading and comments on the manuscript. This work was supported by the Muscular Dystrophy Association (USA) and the Federation Foundation of Greater Philadelphia. B.B. is an investigator of the FRSQ. G.A.R. is supported by the CIHR.

REFERENCES

1. Brais, B., Rouleau, G.A., Bouchard, J.P., Fardeau, M. and Tome, F.-M. (1999) Oculopharyngeal muscular dystrophy. *Semin. Neurol.*, **19**, 59–66.
2. Muller, T., Schroder, R. and Zierz, S. (2001) GCG repeats and phenotype in oculopharyngeal muscular dystrophy. *Muscle Nerve*, **24**, 120–122.
3. Blumen, S.C., Korczyn, A.D., Lavoie, H., Medynski, S., Chapman, J., Asherov, A., Nisipeanu, P., Inzelberg, R., Carasso, R.L., Bouchard, J.P. *et al*. (2000) Oculopharyngeal MD among Bukhara Jews is due to a founder (GCG)9 mutation in the PABP2 gene. *Neurology*, **55**, 1267–1270.
4. Nagashima, T., Kato, H., Kase, M., Maguchi, S., Mizutani, Y., Matsuda, K., Chuma, T., Mano, Y., Goto, Y., Minami, N. *et al*. (2000) Oculopharyngeal muscular dystrophy in a Japanese family with a short GCG expansion (GCG)(11) in PABP2 gene. *Neuromusc. Disord.*, **10**, 173–177.
5. Mirabella, M., Silvestri, G., Di Giovanni, S., Di Muzio, A., Uncini, A., Tonali, P. and Servidei, S. (2000) GCG genetic expansions in Italian patients with oculopharyngeal muscular dystrophy. *Neurology*, **54**, 608–614.
6. Grewal, R.P., Karkera, J.D., Grewal, R.K. and Detera-Wadleigh, S.D. (1999) Mutation analysis of oculopharyngeal muscular dystrophy in Hispanic American families. *Arch. Neurol.*, **56**, 1378–1381.
7. Tome, F.M. and Fardeau, M. (1980) Nuclear inclusions in oculopharyngeal dystrophy. *Acta Neuropathol. (Berl.)*, **49**, 85–87.
8. Tome, F.M., Chateau, D., Helbling-Leclerc, A. and Fardeau, M. (1997) Morphological changes in muscle fibers in oculopharyngeal muscular dystrophy. *Neuromusc. Disord.*, **7**, (Suppl. 1), S63–S69.
9. Brais, B., Xie, Y.G., Sanson, M., Morgan, K., Weissenbach, J., Korczyn, A.D., Blumen, S.C., Fardeau, M., Tome, F.M., Bouchard, J.P. and Rouleau, G.A. (1995) The oculopharyngeal muscular dystrophy locus maps to the region of the cardiac alpha and beta myosin heavy chain genes on chromosome 14q11.2-q13. *Hum. Mol. Genet.*, **4**, 429–434.
10. Brais, B., Bouchard, J.P., Gosselin, F., Xie, Y.G., Fardeau, M., Tome, F.M. and Rouleau, G.A. (1997) Using the full power of linkage analysis in 11 French Canadian families to fine map the oculopharyngeal muscular dystrophy gene. *Neuromusc. Disord.*, **7**, (Suppl. 1), S70–S74.
11. Xie, Y.G., Rochefort, D., Brais, B., Howard, H., Han, F.Y., Gou, L.P., Maciel, P., The, B.T., Larsson, C. and Rouleau, G.A. (1998) Restriction map of a YAC and cosmid contig encompassing the oculopharyngeal muscular dystrophy candidate region on chromosome 14q11.2-q13. *Genomics*, **52**, 201–204.
12. Brais, B., Bouchard, J.P., Xie, Y.G., Rochefort, D.L., Chretien, N., Tome, F.M., Lafreniere, R.G., Rommens, J.M., Uyama, E., Nohira, O. *et al*. (1998) Short GCG expansions in the PABP2 gene cause oculopharyngeal muscular dystrophy. *Nat. Genet.*, **18**, 164–167.
13. Muragaki, Y., Mundlos, S., Upton, J. and Olsen, B.R. (1996) Altered growth and branching patterns in synpolydactyly caused by mutations in HOXD13. *Science*, **272**, 548–551.
14. Mundlos, S., Otto, F., Mundlos, C., Mulliken, J.B., Aylsworth, A.S., Albright, S., Lindhout, D., Cole, W.G., Henn, W., Knoll, J.H. *et al*. (1997) Mutations involving the transcription factor CBFA1 cause cleidocranial dysplasia. *Cell*, **89**, 773–779.
15. Brown, S.A., Warburton, D., Brown, L.Y., Yu, C.Y., Roeder, E.R., Stengel-Rutkowski, S., Hennekam, R.C.M. and Muenke, M. (1998) Holoprosencephaly due to mutations in ZIC2, a homologue of *Drosophila* odd-paired. *Nat. Genet.*, **20**, 180–183.
16. Goodman, F.R., Bacchelli, C., Brady, A.F., Brueton, L.A., Fryns, J.P., Mortlock, D.P., Innis, J.W., Holmes, L.B., Donnenfeld, A.E., Feingold, M. *et al*. (2000) Novel HOXA13 mutations and the phenotypic spectrum of hand-foot-genital syndrome. *Am. J. Hum. Genet.*, **67**, 197–202.
17. Crisponi, L., Deiana, M., Loi, A., Chiappe, F., Uda, M., Amati, P., Bisceglia, L., Zelante, L., Nagaraja, R., Porcu, S. *et al*. (2001) The putative

forkhead transcription factor FOXL2 is mutated in blepharophimosis/ptosis/epicanthus inversus syndrome. *Nat. Genet.*, **27**, 159–166.
18. Ferrigno, P. and Silver, P.A. (2000) Polyglutamine expansions: proteolysis, chaperones, and the dangers of promiscuity. *Neuron*, **26**, 9–12.
19. Huntington's Disease Collaborative Research Group (1993) A novel gene containing a trinucleotide repeat that is expanded and unstable on Huntington's disease chromosomes. *Cell*, **72**, 971–983.
20. La Spada, A.R., Wilson, E.M., Lubahn, D.B., Harding, A.E. and Fischbeck, K.H. (1991) Androgen receptor gene mutations in X-linked spinal and bulbar muscular atrophy. *Nature*, **352**, 77–79.
21. Koide, R., Ikeuchi, T., Onodera, O., Tanaka, H., Igarashi, S., Endo, K., Takahashi, H., Kondo, R., Ishikawa, A., Hayashi, T. *et al.* (1994) Unstable expansion of CAG repeat in hereditary dentatorubral-pallidoluysian atrophy (DRPLA). *Nat. Genet.*, **6**, 9–13.
22. Nagafuchi, S., Yanagisawa, H., Sato, K., Shirayama, T., Ohsaki, E., Bundo, M., Takeda, T., Tadokoro, K., Kondo, I., Murayama, N. *et al.* (1994) Dentatorubral and pallidoluysian atrophy expansion of an unstable CAG trinucleotide on chromosome 12p. *Nat. Genet.*, **6**, 14–18.
23. Orr, H.T., Chung, M.Y., Banfi, S., Kwiatowski, T.J., Servadio, A., Beaudet, A.L., McCall, A.E., Duvick, L.A., Ranum, L.P. and Zoghbi, H.Y. (1993) Expansion of an unstable trinucleotide CAG repeat in spinocerebellar ataxia type 1. *Nat. Genet.*, **4**, 221–226.
24. Kawaguchi, Y., Okamoto, T., Taniwaki, M., Aizawa, M., Inoue, M., Katayama, S., Kawakami, H., Nakamura, S., Nishmura, M., Akiguchi, I. *et al.* (1994) CAG expansions in a novel gene for Machado-Joseph disease at chromosome 14q32.1. *Nat. Genet.*, **8**, 221–228.
25. Imbert, G., Saudou, F., Yvert, G., Devys, D., Trottier, Y., Garnier, J.M., Weber, C., Mandel, J.L., Cancel, G., Abbas, N. *et al.* (1996) Cloning of the gene for spinocerebellar ataxia 2 reveals a locus with high sensitivity to expanded CAG/glutamine repeats. *Nat. Genet.*, **14**, 285–291.
26. Pulst, S.M., Nechiporuk, A., Nechiporuk, T., Gispert, S., Chen, X.N., Lopes-Cendes, I., Pearlman, S., Starkman, S., Orozco-Diaz, G., Lunkes, A. *et al.* (1996) Moderate expansion of a normally biallelic trinucleotide repeat in spinocerebellar ataxia type 2. *Nat. Genet.*, **14**, 269–276.
27. Sanpei, K., Takano, H., Igarashi, S., Sato, T., Oyake, M., Sasaki, H., Wakisaka, A., Tashiro, K., Ishida, Y., Ikeuchi, T. *et al.* (1996) Identification of the spinocerebellar ataxia type 2 gene using a direct identification of repeat expansion and cloning technique, DIRECT. *Nat. Genet.*, **14**, 277–284.
28. David, G., Abbas, N., Stevanin, G., Durr, A., Yvert, G., Cancel, G., Weber, C., Imbert, G., Saudou, F., Antoniou, E. *et al.* (1997) Cloning of the SCA7 gene reveals a highly unstable CAG repeat expansion. *Nat. Genet.*, **17**, 65–70.
29. Koob, M.D., Benzow, K.A., Bird, T.D., Day, J.W., Moseley, M.L. and Ranum, L.P. (1998) Rapid cloning of expanded trinucleotide repeat sequences from genomic DNA. *Nat. Genet.*, **18**, 72–75.
30. Wahle, E. (1991) A novel poly(A)-binding protein acts as a specificity factor in the second phase of messenger RNA polyadenylation. *Cell*, **66**, 759–768.
31. Colgan, D.F. and Manley, J.L. (1997) Mechanism and regulation of mRNA polyadenylation. *Genes Dev.*, **11**, 2755–2766.
32. Minvielle-Sebastia, L. and Keller, W. (1999) mRNA polyadenylation and its coupling to other RNA processing reactions and to transcription. *Curr. Opin. Cell Biol.*, **11**, 352–357.
33. Barabino, S.M.L. and Keller, W. (1999) Last but not least: regulated poly(A) tail formation. *Cell*, **99**, 9–11.
34. Wahle, E. (1995) Poly(A) tail length control is caused by termination of processive synthesis. *J. Biol. Chem.*, **270**, 2800–2808.
35. Bienroth, S., Keller, W. and Wahle, E. (1993) Assembly of a processive messenger RNA polyadenylation complex. *EMBO J.*, **12**, 585–594.
36. Wahle, E., Lusting, A., Jeno, P. and Maurer, P. (1993) Mammalian poly(A)-binding protein II. Physical properties and binding to polynucleotides. *J. Biol. Chem.*, **268**, 2937–2945.
37. Keller, R.W., Kuhn, U., Aragon, M., Bornikova, L., Wahle, E. and Bear, D.G. (2000) The nuclear poly(A) binding protein, PABP2, forms an oligomeric particle covering the length of the poly(A) tail. *J. Mol. Biol.*, **297**, 569–583.
38. Nemeth, A., Krause, S., Blank, D., Jenny, A., Jeno, P., Lusting, A. and Wahle, E. (1995) Isolation of genomic and cDNA clones encoding bovine poly(A) binding protein II. *Nucleic Acids Res.*, **23**, 4034–4041.
39. Calado, A., Tome, F.M.S., Brais, B., Rouleau, G.A., Kuhn, U., Wahle, E. and Carmo-Fonseca, M. (2000) Nuclear inclusions in oculopharyngeal muscular dystrophy consist of poly(A) binding protein 2 aggregates which sequester poly(A) RNA. *Hum. Mol. Genet.*, **9**, 2321–2328.
40. Becher, M.W., Kotzuk, J.A., Davis, L.E. and Bear, D.G. (2000) Intranuclear inclusions in oculopharyngeal muscular dystrophy contain poly(A) binding protein 2. *Ann. Neurol.*, **48**, 812–815.
41. Uyama, E., Tsukahara, T., Goto, K., Kurano, Y., Ogawa, M., Kim, Y.J., Uchino, M. and Arahata, K. (2000) Nuclear accumulation of expanded PABP2 gene product in oculopharyngeal muscular dystrophy. *Muscle Nerve*, **23**, 1549–1554.
42. Shanmugam, V., Dion, P., Rochefort, D., Laganiere, J., Brais, B. and Rouleau, G.A. (2000) PABP2 polyalanine tract expansion causes intranuclear inclusions in oculopharyngeal muscular dystrophy. *Ann. Neurol.*, **48**, 798–802.
43. Kim, Y.J., Noguchi, S., Hayashi, Y.K., Tsukahara, T., Shimizu, T. and Arahata, K. (2001) The product of an oculopharyngeal muscular dystrophy gene, poly(A)-binding protein 2, interacts with SKIP and stimulates muscle-specific gene expression. *Hum. Mol. Genet.*, **10**, 1129–1139.
44. Rankin, J., Wyttenbach, A. and Rubinsztein, D.C. (2000) Intracellular green fluorescent protein-polyalanine aggregates are associated with cell death. *Biochem. J.*, **348**, 15–19.
45. Krause, S., Fakan, S., Weis, K. and Wahle, E. (1994) Immunodetection of poly(A) binding protein II in the cell nucleus. *Exp. Cell Res.*, **214**, 75–82.
46. Calado, A. and Carmo-Fonseca, M. (2000) Localization of poly(A)-binding protein 2 (PABP2) in nuclear speckles is independent of import into the nucleus and requires binding to poly(A) RNA. *J. Cell Sci.*, **113**, 2309–2318.
47. Ferrigno, P. and Silver, P.A. (2000) Polyglutamine expansions: proteolysis, chaperones, and the dangers of promiscuity. *Neuron*, **26**, 9–12.
48. Sherman, M.Y. and Goldberg, A.L. (2001) Cellular defenses against unfolded proteins: a cell biologist thinks about neurodegenerative diseases. *Neuron*, **29**, 15–32.
49. Bates, G.P., Mangiarini, L. and Davies, S.W. (1998) Transgenic mice in the study of polyglutamine repeat expansion diseases. *Brain Pathol.*, **8**, 699–714.
50. Yong, A. (1998) In Martin, J. (ed.), *Huntington's Disease and Other Trinucleotide Repeat Disorders*. Scientific American, Inc., New York, NY.
51. Saudou, F., Finkbeiner, S., Devys, D. and Greenberg, M.E. (1998) Huntingtin acts in the nucleus to induce apoptosis but death does not correlate with the formation of intranuclear inclusions. *Cell*, **95**, 55–66.
52. Klement, I.A., Skinner, P.J., Kaytor, M.D., Yi, H., Hersch, S.M., Clark, H.B., Zoghbi, H.Y. and Orr, H.T. (1998) Ataxin-1 nuclear localization and aggregation: role in polyglutamine-induced disease in SCA1 transgenic mice. *Cell*, **95**, 41–53.
53. Evert, B.O., Wullner, U., Schulz, J.B., Weller, M., Groscurth, P., Trottier, Y., Brice, A. and Klockgether, T. (1999) High level expression of expanded full-length ataxin-3 *in vitro* causes cell death and formation of intranuclear inclusions in neuronal cells. *Hum. Mol. Genet.*, **8**, 1169–1176.
54. Turmaine, M., Raza, A., Mahal, A., Mangiarini, L., Bates, G.P. and Davies, S.W. (2000) Nonapoptotic neurodegeneration in a transgenic mouse model of Huntington's disease. *Proc. Natl Acad. Sci. USA*, **97**, 8089–8097.
55. Anton, L.C., Schubert, U., Bacik, I., Princiotta, M.F., Wearsch, P.A., Gibbs, J., Day, P.M., Realini, C., Rechsteriner, M.C., Bennink, J.R. and Yewdell, J.W. (1999) Intracellular localization of proteasomal degradation of a viral antigen. *J. Cell Biol.*, **146**, 113–124.
56. Johnston, J.A., Ward, C.L. and Kopito, R.R. (1998) Aggresomes: a cellular response to misfolded proteins. *J. Cell Biol.*, **143**, 1883–1898.
57. Garcia-Mata, R., Bebok, Z., Sorscher, E.J. and Sztul, E.S. (1999) Characterization and dynamics of aggresome formation by a cytosolic GFP-chimera. *J. Cell Biol.*, **146**, 1239–1254.